



The effect of enhancement factor on the angular dependence of L x-ray intensity ratios for Sm, Hf, Pb and U

Tuba Akkuş^{a,*}, Demet Yılmaz^b, Mine Uğurlu^b

^a Department of Physics, Faculty of Arts and Sciences, Erzincan Binali Yıldırım University, Erzincan, 24100, Turkey

^b Department of Physics, Faculty of Sciences, Ataturk University, Erzurum, 25240, Turkey

ARTICLE INFO

Keywords:

Enhancement factor
L X-rays
Angular dependence

ABSTRACT

The effect of enhancement factor on the angular dependence of L_1/L_γ , L_α/L_γ and L_β/L_γ X-ray intensity ratios for Sm, Hf, Pb and U elements have been measured by using the 59.54 keV photon energy. The binary systems are prepared as Sm-CeO₂, Hf-CeO₂, Pb-CeO₂ and U-CeO₂. The samples have been analyzed in EDXRF system. The measurements are made in scattering angles of 85°, 95°, 105°, 115° and 125°. The L X-ray spectra from different samples were detected by a Si(Li) detector. The results show that the intensity ratios of L X-rays to be greater than expected due to the enhancement effect.

1. Introduction

The EDXRF technique is an efficient method for elemental analysis and widely used in pharmacy, medicine, industry, archeology and many other fields. In the EDXRF technique, since each of the elements within the sample emits X-rays in their characteristic energies, and the number of these rays is proportional to the concentration of that element in the sample, qualitative and quantitative analyzes are based on the presence of energies and counts of these characteristic X-rays. The intensity of the characteristic X-rays of the elements emitted by the sample varies depending on the composition of the element, the thickness of the sample, the experimental geometry, the activity of the source, the efficiency of the detector and the effects of the matrix.

The analyte is called the element examined in a sample. The other elements of the samples (except analyte) are called matrix. The effects of other elements on the analyte intensity is usually referred to as matrix effects. The absorption and enhancement phenomenons are matrix effects in XRF and are very important parameters in XRF. The analyte line can be affected by matrix and expected results cannot be obtained. In this case intensity is higher than expected. The enhancement effect is caused by atoms that are excited not by the tube (or radioactive source) but by X-rays from a neighboring atom. If the energy of the characteristic X-rays emitted by the matrix elements in the sample is greater than the absorption edge of the analyte, they can excite the analyte in addition to the primary exciting photons. This is defined as the enhancement effect of the matrix. The matrix effect should be calculated especially in the analysis of X-ray fluorescence of

geological and biological samples.

Criss and Birks (1968) developed the method used to correct matrix effects. Mainardi et al. (1982) used semi-experimental correlations to calculate the enhancement effect. Broll (1986) investigated the effect of exacerbation in X-ray fluorescence analysis using the method of fundamental effect coefficient. Counture and Dymek (1996) investigated absorption and enhancement effects in X-ray fluorescence trace element analysis. Tıraşoğlu and Ertuğrul (1998) measured enhancement effect factors at 59.54 keV photon energy. Söğüt et al. (2002) investigated chemical effects on enhancement of Coster-Kronig transition of L_3 X-rays of Hg, Pb and Bi compounds. Han et al. (2006) studied the enhancement effects in X-ray fluorescence analysis for multi-layer samples. Söğüt (2006) investigated Coster-Kronig enhancement effect for L_3 subshell X-rays using the experimental L_α X-ray production cross-section. Yılmaz et al. (2009) investigated Coster-Kronig enhancement factors for Yb, Lu, Os and Pt elements and they found the experimental enhancement factors tend to be smaller than those predicted by theory.

In this work, the effect of enhancement factor on the angular dependence of L x-ray intensity ratios for Sm, Hf, Pb and U was investigated at 59.54 keV photon energy. Sm, Hf, Pb and U are chosen as analyte. Also, Sm-CeO₂, Hf-CeO₂, Pb-CeO₂ and U-CeO₂ are matrix for this study.

* Corresponding author.

E-mail address: takkus@erzincan.edu.tr (T. Akkuş).

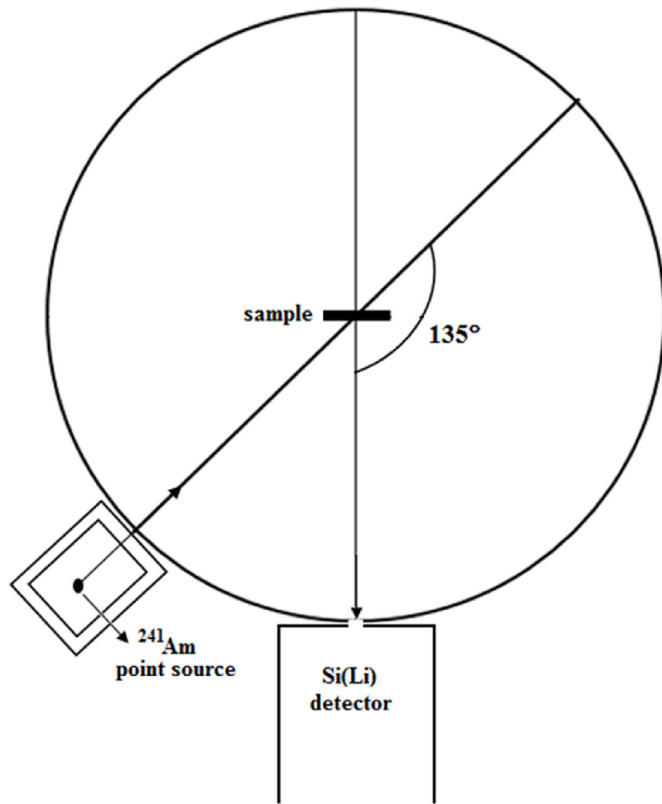


Fig. 1. Experimental geometry.

2. Materials and methods

2.1. Experimental details

In this study, a Si (Li) detector with a resolution of 160 eV at 5.9 keV was used for XRF measurements. The samples were irradiated with ^{241}Am point source. The data were acquired into 4096 channels of the multichannel analyzer. Genie-2000 program was used to acquire the spectra and to control the operating parameters of the system. The analysis of peak areas was done by Origin 9.1 Software program. In experimental geometry, the scattering angle (θ) was changed from 85° to 125° with 10° steps by moving the source and the sample together, keeping the angle of the gamma rays from the point source to 45° with the sample normal. Thus, the measurements were made in scattering angles of 85° , 95° , 105° , 115° and 125° . In all measurements, the symmetry axes of the source and detector were aligned with the sample center. To change the scattering angles, the detector was held in a fixed position and the movement of the source and sample placed on a goniometer was ensured. The experimental geometry is given in Fig. 1. A linear background function was selected for the analysis of L X-ray peaks. The background count rate was subtracted from all the measurements. The pulse height spectrum for each sample was acquired for a period of 6 h.

In this study, binary systems of Sm-CeO_2 , Hf-CeO_2 , Pb-CeO_2 and U-CeO_2 were prepared. The concentrations of analyte and matrix were 95% and 5%, respectively. The powdered samples were weighed with a scale of 10^{-5} g of sensitivity. Analyte and matrix were mixed in mixer for 10 min to ensure a uniform distribution of cerium oxide. A hydraulic press of 8 ton was used to perform a thin pellet of 0.65 cm radius. The typical spectrum of Pb-CeO_2 acquired with the detection system are shown in Fig. 2. As can be seen from Fig. 2, the peaks due to the $L\alpha$, $L\beta$ and $L\gamma$ group of lines are well resolved.

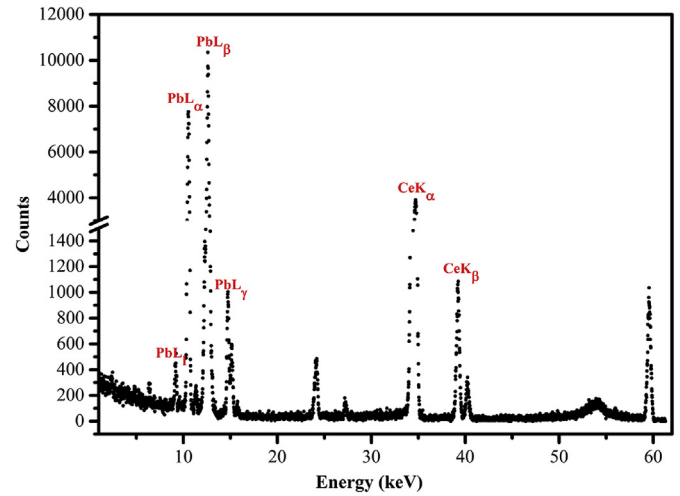


Fig. 2. The typical spectrum of Pb-CeO_2 .

2.2. Theoretical details

2.2.1. Determination of L X-ray intensity ratios

The experimental L x-ray intensity ratio at a scattering angle can be given as

$$\frac{I_k}{I_y} = \frac{N_{Lk}(\theta) \beta_{Ly}(\theta) \varepsilon_{Ly}(\theta)}{N_{Ly}(\theta) \beta_{Lk}(\theta) \varepsilon_{Lk}(\theta)} \quad (1)$$

where $N_{Lk}(\theta)$ is the number of L x-rays detected per second in the L_k X-ray peak at an angle θ for the photon energy, $\varepsilon_{Lk}(\theta)$ is the efficiency of the detector for the detection of X-rays emitted at angle θ and $\beta_{Lk}(\theta)$ is the target self-absorption correction factor. The self-absorption correction factor can be calculated by following equation

$$\beta_{Lk}(\theta) = \frac{1 - \exp[-(\mu_{inc}/\cos\theta_1 + \mu_{emt}/\cos\theta_2)t]}{(\mu_{inc}/\cos\theta_1 + \mu_{emt}/\cos\theta_2)t} \quad (2)$$

where μ_{inc} and μ_{emt} are the attenuation coefficients ($\text{cm}^2 \text{g}^{-1}$) of the incident photons and emitted characteristic X-rays, respectively, θ_1 and θ_2 are the angles of incident photon and emitted X-ray with the target. In this work, WinXCom program was used to obtain μ_{inc} and μ_{emt} (Gerward et al., 2004).

The effective incident photon flux factor $I_0 G \varepsilon$ was determined by using the following relation (Akkuş et al., 2017).

$$I_0 G \varepsilon_{K\alpha} = \frac{N_{K\alpha}}{\sigma_{K\alpha} t \beta_{K\alpha}} \quad (3)$$

where $I_0 G \varepsilon_{K\alpha}$, $N_{K\alpha}$, $\sigma_{K\alpha}$ are the effective photon flux of the relevant K_α , the number of counts under the K_α peak and fluorescence cross section for the K_α peaks respectively. I_0 is the intensity of incident radiation, G is the geometrical factor.

In this work, K x-rays were measured from pure targets in the atomic range $23 \leq Z \leq 42$ (V, Mn, Co, Ni, Cu, Zn, Y, Zr, Nb ve Mo) to determine $I_0 G \varepsilon$ factor.

2.2.2. Determination of enhancement factor

If the excitation source is monochromatic (emits only one energy), the intensity of the fluorescent radiation $I_i(E_i)$ is described by following equation (Grieken and Markowicz, 2001)

$$I_i(E_i) = G \frac{\varepsilon(E_i) a_i(E_0) I_0(E_0)}{\sin\theta_1} \frac{1 - \exp[-pT(\mu(E_0)\csc\theta_1 + \mu(E_i)\csc\theta_2)]}{\mu(E_0)\csc\theta_1 + \mu(E_i)\csc\theta_2} \quad (4)$$

The enhancement effect, consisting of an extra excitation of the element of interest by the characteristic radiation of some matrix elements, modifies the equations for the intensity $I_i(E_i)$.

In the case of monochromatic photon excitation, a factor, $1 + H_i$ should be included in Eq. (4):

$$H_i = \frac{1}{2\mu_i(E_0)} \sum_{k=1}^m W_k w_k \left(1 - \frac{1}{J_k} \right) \mu_i(E_k) \mu_k(E_0) \times \left[\frac{\ln(1 + \mu(E_0)/[\mu(E_k)\text{Sin } \theta_1])}{\mu(E_0)/\text{Sin } \theta_1} + \frac{\ln(1 + \mu(E_i)/[\mu(E_k)\text{Sin } \theta_2])}{\mu(E_i)/\text{Sin } \theta_2} \right] \tag{5}$$

where H_i is enhancement term, $\mu_i(E_0)$ and $\mu_i(E_k)$ are total mass attenuation coefficients for the analyte at the incident radiation energy and at the energy of characteristic X-ray energy of the matrix element, respectively. $\mu_k(E_0)$ and $\mu(E_0)$ are the total mass attenuation coefficient for the matrix element and sample at the energy of incident radiation, respectively. $\mu(E_k)$ and $\mu(E_i)$ are the total mass attenuation for samples at the energy of characteristic X-ray energy of the matrix element and at the energy of incident radiation, respectively. W_k and w_k are the mass fraction and fluorescent yield of the matrix element, respectively. J_k is the absorption edge jump ratio of the matrix element. θ_1 and θ_2 are the angles of incident photon and emitted X-ray from the target. New intensity relation can be given due to the enhancement term as:

$$I_{i+k}(E_{i+k}) = I_i(E_i)(1 + H_i) \tag{6}$$

3. Results and discussion

The energy of the *K* X-rays emitted by the cerium in the investigated samples are greater than the *L* X-ray energies of the each analyte. *K* X-rays of cerium excite the *L* x-rays of the analyte. Therefore, the intensity is higher than expected. Thus, the contribution of the enhancement factor should be taken into account when calculating the intensity ratios. In this study, the values of enhancement factor have been calculated using Eq. (4). L_i/L_γ , L_α/L_γ and L_β/L_γ X-ray intensity ratios for Sm, Hf, Pb and U have been calculated by using Eq. (1). and given in Table 1a, Table 2a, Table 3a and Table 4a, respectively. The intensity ratios calculated by taking into account enhancement factors was given in Table 1b, Table 2b, Table 3b and Table 4b for the investigated samples.

Relative differences between maximum value and minimum value were calculated by relation $\text{diff. } (\%) = |(A - B/A) * 100|$. As can be seen from Tables 1a-Table 4a, $\text{diff. } \% = [(A - B)/A]*100$ relative differences in the L_i/L_γ intensity ratios with scattering angles are in the range 25.97–30.56%. Relative differences in the L_α/L_γ intensity ratios for all scattering angles are in the range 3.55–23.99%. Also, relative differences in the L_β/L_γ intensity ratios with scattering angles in the range 0.52–8.16%. As seen from these result, the weakest angular dependence of *L* x-rays relative intensity ratio is that of L_β/L_γ .

As seen from Tables 1a–1b, Tables 2a–2b, Tables 3a–3b and Tables 4a–4b, L_i/L_γ , L_α/L_γ and L_β/L_γ X-ray intensity ratios for Sm, Hf, Pb and U increase with taking into account the enhancement factors. The enhancement factor was effective at least at L_β/L_γ intensity ratio for Sm. Also, the enhancement factor was effective at most at L_i/L_γ intensity ratio for U. $\text{diff. } \% = [(A - B)/A]*100$ Relative differences in the L_i/L_γ , L_α/L_γ and L_β/L_γ intensity ratios increase with the increasing atomic number in the investigated angular range.

By measuring the energy and intensity characteristics of x-rays in

Table 1a
The angular dependence of L_i/L_γ , L_α/L_γ and L_β/L_γ intensity ratios for Sm-CeO₂.

Scattering angle, θ	L_i/L_γ	L_α/L_γ	L_β/L_γ
85°	0.191	4.787	5.587
95°	0.179	4.719	5.728
105°	0.169	4.679	5.919
115°	0.162	4.678	6.186
125°	0.141	4.617	6.043

Table 1b
The effect of enhancement factor on the angular dependence of L_i/L_γ , L_α/L_γ and L_β/L_γ for Sm-CeO₂.

Scattering angle, θ	L_i/L_γ	L_α/L_γ	L_β/L_γ
85°	0.200	4.958	5.716
95°	0.187	4.868	5.845
105°	0.175	4.802	6.020
115°	0.166	4.771	6.266
125°	0.143	4.671	6.090

Table 2a
The angular dependence of L_i/L_γ , L_α/L_γ and L_β/L_γ intensity ratios for Hf-CeO₂.

Scattering angle, θ	L_i/L_γ	L_α/L_γ	L_β/L_γ
85°	0.156	3.570	4.952
95°	0.132	3.429	4.895
105°	0.126	3.385	5.010
115°	0.118	3.269	5.026
125°	0.110	3.217	5.032

Table 2b
The effect of enhancement factor on the angular dependence of L_i/L_γ , L_α/L_γ and L_β/L_γ for Hf-CeO₂.

Scattering angle, θ	L_i/L_γ	L_α/L_γ	L_β/L_γ
85°	0.167	3.771	5.114
95°	0.141	3.602	5.039
105°	0.133	3.531	5.137
115°	0.123	3.378	5.125
125°	0.113	3.283	5.094

Table 3a
The angular dependence of L_i/L_γ , L_α/L_γ and L_β/L_γ intensity ratios for Pb-CeO₂.

Scattering angle, θ	L_i/L_γ	L_α/L_γ	L_β/L_γ
85°	0.301	6.382	6.297
95°	0.261	6.047	6.272
105°	0.234	5.463	6.311
115°	0.221	5.009	6.255
125°	0.209	4.851	6.330

Table 3b
The effect of enhancement factor on the angular dependence of L_i/L_γ , L_α/L_γ and L_β/L_γ for Pb-CeO₂.

Scattering angle, θ	L_i/L_γ	L_α/L_γ	L_β/L_γ
85°	0.341	7.033	6.637
95°	0.293	6.614	6.586
105°	0.259	5.914	6.592
115°	0.240	5.342	6.483
125°	0.220	5.060	6.483

Table 4a
The angular dependence of L_i/L_γ , L_α/L_γ and L_β/L_γ intensity ratios for U-CeO₂.

Scattering angle, θ	L_i/L_γ	L_α/L_γ	$L_{\beta 2,4}/L_\gamma$	$L_{\beta 1,3}/L_\gamma$
85°	0.258	3.391	1.078	2.327
95°	0.246	3.440	1.099	2.368
105°	0.225	3.356	1.031	2.378
115°	0.207	3.243	1.024	2.284
125°	0.191	3.014	1.018	2.247

Table 4b

The effect of enhancement factor on the angular dependence of L_I/L_γ , L_α/L_γ , $L_{\beta_{2,4}}/L_\gamma$ and $L_{\beta_{1,3}}/L_\gamma$ for U-CeO₂.

Scattering angle, θ	L_I/L_γ	L_α/L_γ	$L_{\beta_{2,4}}/L_\gamma$	$L_{\beta_{1,3}}/L_\gamma$
85°	0.312	3.917	1.167	2.480
95°	0.294	3.946	1.186	2.517
105°	0.265	3.807	1.107	2.518
115°	0.237	3.613	1.089	2.401
125°	0.210	3.254	1.065	2.331

EDXRF, the element type, atomic parameters and concentration for unknown samples could be determined. However, a difference exists between the standard sample and unknown sample, such as physical structure, chemical composition and so on. Thus, there would be some deviations in the EDXRF results. This is called the matrix (absorption and enhancement) effect. Self-absorption correction factor is calculated for experimental studies on angular dependence of x-rays. This study is shown that enhancement also affect the angular dependence of L x-ray intensity ratios. The results obtained will guide to studies in which the L x-ray intensity ratios versus analyte concentration will be plotted, calibration curve will be determined, and fit equation will be calculated. Thus, more accuracy results can be obtained for alignment and polarization parameters, anisotropy and angular dependence of x-ray.

4. Conclusions

In the present work, the effect of enhancement factor on the angular dependence of L_I/L_γ , L_α/L_γ and L_β/L_γ X-ray intensity ratios for Sm, Hf, Pb and U elements have been investigated. The measurements have been done by using 59.54 keV photon energy and a Si(Li) detector in EDXRF system. In studies on the angular distribution of X-rays, it is

necessary to investigate the change in intensity due to the change of scattering angle. A different element can be added to the sample when investigating the angular distribution of L X-rays with control or reference purposes. Also, the investigated sample may not be pure. The X-rays of selected reference element can excite the L X-rays of the analyte. Therefore, the intensity is higher than expected. Thus, the contribution of the enhancement factor should be taken into account when calculating the atomic parameters (intensity, intensity ratios, fluorescence cross-section, fluorescence yields, etc.).

References

- Akkus, T., Alim, B., Yilmaz, D., Şahin, Y., 2017. L-shell differential cross-section and alignment of uranium at 59.54-keV photon energy. *Appl. Radiat. Isot.* 130, 60–65.
- Broll, N., 1986. Quantitative x-ray fluorescence analysis. Theory and practice of the fundamental coefficient method. *X Ray Spectrom.* 15, 271–285.
- Counture, R.A., Dymek, R.F., 1996. A reexamination of absorption and enhancement effects in X-ray fluorescence trace element analysis. *Am. Mineral.* 81 (5–6), 639–650.
- Criss, J.W., Birks, L.S., 1968. Calculation methods for fluorescent X-ray spectrometry. *Anal. Chem.* 40 (7), 1080–1086.
- Gerward, L., Guilbert, N., Jensen, K.B., Levring, H., 2004. WinXCom-a program for calculating X-ray attenuation coefficients. *Radiat. Phys. Chem.* 71, 653–654.
- Grieken, R.E.V., Markowicz, A.A., 2001. *Handbook of X-Ray Spectrometry.* (New York.).
- Han, X.Y., Zhuo, S.J., Wang, P.L., 2006. Study of enhancement effects in X-ray fluorescence analysis for multi-layer samples. *Spectrosc. Spectr. Anal.* 26 (2), 353–357.
- Mainardi, R.T., Fernandez, J.E., Nores, M., 1982. Influence of interelement effects on x-ray fluorescence calibration curve coefficients for binary mixtures. *X Ray Spectrom.* 11 (2), 70–78.
- Söğüt, Ö., Büyükkasap, E., Ertuğrul, M., Küçükönder, A., 2002. Chemical effect on enhancement of Coster-Kronig transition of L-3 X-rays. *J Quant Spectrosc RA* 74 (3), 395–400.
- Söğüt, Ö., 2006. Variation of enhancement effect of Coster-Kronig transition of L-3 X-Rays of Ba, La and Ce compounds. *J Quant Spectrosc Ra* 97 (3), 388–394.
- Tıraşoğlu, E., Ertuğrul, M., 1998. Measurement of the enhancement effect in different series in X-ray fluorescence analysis. *J. Radioanal. Nucl. Chem.* 237 (1–2), 147–150.
- Yılmaz, R., Öz, E., Tan, M., Durak, R., Şahin, Y., 2009. Measurements of Coster-Kronig enhancement factors for Yb, Lu, Os and Pt elements. *Radiat. Phys. Chem.* 78 (5), 318–322.